LA-UR-20-21569 (Accepted Manuscript)

Extraction chromatography of 225Ac and lanthanides on N,N-dioctyldiglycolamic acid /1-butyl-3-methylimidazolium bis(trifluoromethylsulfonyl)imide solvent impregnated resin

Friend, Mitchell Thomas
Parker, Tracey Gannon
Mastren, Tara
Mocko, Veronika
Brugh, Mark
Birnbaum, Eva R.
Fassbender, Michael Ernst

To be published in: Journal of Chromatography A

DOI to publisher's version: 10.1016/j.chroma.2020.461219

Permalink to record: http://permalink.lanl.gov/object/view?what=info:lanl-repo/lareport/LA-UR-20-21569

Extraction chromatography of ^{225}Ac and lanthanides on N,N-dioctyldiglycolamic acid /1-butyl-3-methylimidazolium bis(trifluoromethylsulfonyl)imide solvent impregnated resin

Mitchell T. Friend , T. Gannon Parker , Tara Mastren , Veronika Mocko , Mark Brugh , Eva R. Birnbaum , Michael E. Fassbender

PII: S0021-9673(20)30481-7
DOI: https://doi.org/10.1016/j.chroma.2020.461219
Reference: CHROMA 461219

To appear in: *Journal of Chromatography A*

Received date: 19 February 2020
Revised date: 5 May 2020
Accepted date: 7 May 2020

Please cite this article as: Mitchell T. Friend , T. Gannon Parker , Tara Mastren , Veronika Mocko , Mark Brugh , Eva R. Birnbaum , Michael E. Fassbender , Extraction chromatography of ^{225}Ac and lanthanides on N,N-dioctyldiglycolamic acid /1-butyl-3-methylimidazolium bis(trifluoromethylsulfonyl)imide solvent impregnated resin, *Journal of Chromatography A* (2020), doi: https://doi.org/10.1016/j.chroma.2020.461219

Extraction chromatography of ^{225}Ac and lanthanides on *N*,*N*-dioctyldiglycolamic acid DODGAA/1-butyl-3-methylimidazolium bis(trifluoromethylsulfonyl)imide [Bmin][NTf$_2$] solvent impregnated resin

Mitchell T. Friend[1,†], T. Gannon Parker[1,†], Tara Mastren[1,2], Veronika Mocko[1], Mark Brugh[1], Eva R. Birnbaum[1], and Michael E. Fassbender[1,*]

[1]Chemistry Division, Los Alamos National Laboratory, P.O. Box 1663, Los Alamos, NM 87545, USA

[2]Present address: Nuclear Engineering Program, Department of Civil and Environmental Engineering, University of Utah, 110 Central Campus Drive, Suite 2000b, Salt Lake City, UT 84112, USA

†These authors have contributed equally to this work.

***Corresponding Author**
Michael E. Fassbender
Los Alamos National Laboratory MS J975
Los Alamos, NM 87545
mifa@lanl.gov, radiochemistry@outlook.com
505-665-7306

Keywords: Extraction chromatography, Actinium-225, Lanthanide separation, Ionic liquid, Solvent impregnated resin

Abstract

The alpha-emitter ^{225}Ac ($t_{1/2}$ = 9.92 d) is currently under development for targeted alpha-particle therapy of cancer, and accelerator production of ^{225}Ac via proton irradiation of thorium targets requires robust separations of ^{225}Ac from chemically similar fission product lanthanides. Additionally, the lanthanide elements represent critical components in modern technologies, and radiolanthanides such as ^{140}Nd ($t_{1/2}$ = 3.37 d) also have potential application in the field of nuclear medicine. —The ionic liquid, 1-butyl-3-methylimidazolium bis(trifluoromethylsulfonyl)imide ([Bmim][NTf$_2$]), combined with the diglycolamide extractant, *N*,*N*-dioctyldiglycolamic acid (DODGAA), was adsorbed on macro-porous resin support to produce a solvent impregnated resin (SIR) that was investigated for separations of ^{225}Ac and lanthanides. The equilibrium distribution coefficients (K_d) of the rare earth elements (Sc(III),

Formatted: Font: Bold

Formatted: Font: Bold

Y(III), Ln(III)), ^{225}Ac(III), Th(IV), and U(VI) on the prepared DODGAA/[Bmim][NTf_2]-SIR were determined from batch adsorption experiments in HCl and HNO_3 media. The DODGAA/[Bmim][NTf_2]-SIR exhibited preferential uptake of the heavier lanthanide elements while allowing for the separation of the lighter lanthanides. Column separations utilizing the DODGAA/[Bmim][NTf_2]-SIR were effective at separating the lighter lanthanides from each other, and separating ^{225}Ac from a mixture of lanthanides, ^{213}Bi, and ^{225}Ra without the need for additional complexing agents.

1. Introduction

Targeted alpha-particle therapy (TAT) has been shown in recent years to be a promising route for the treatment of various forms of cancer, and may serve as an alternative to more traditional cancer treatment options [1-4]. A number of alpha-emitting radionuclides are being explored for therapeutic applications including ^{149}Tb, ^{212}Bi, ^{213}Bi, ^{211}At, ^{223}Ra, ^{224}Ra, ^{225}Ac, and others [2,5]. Actinium-225 in particular has proven itself to be an especially appealing isotope for the treatment of some cancers [1,6].

The primary source of ^{225}Ac is from the decay of ^{229}Th ($t_{1/2}$ = 7932 y)~~ (Fig. 1)~~ [7]. Alternatively, ^{225}Ac can be produced via proton irradiation of ^{232}Th, however, this process necessitates the separation of ^{225}Ac from bulk Th as well as a large number of fission products and radiochemical impurities [8-10]. Fission product lanthanides (Ln)—^{140}La, ^{141,143}Ce, ^{147}Nd, and ^{148m}Pm in particular—present a difficult separation from ^{225}Ac due to the chemical similarities that stem from the trivalent oxidation state that is shared by Ln(III) and Ac(III) in solution.

Formatted: Font color: Text 1

Formatted: Font color: Text 1

Several techniques have been developed that addresses the issue of separating the ^{225}Ac from the irradiated Th target matrix in order to isolate clinically relevant amounts of the isotope.

Anion exchange and cation exchange chromatography may be employed to remove bulk Th and main group impurities [2,7,11,12]. Extraction chromatography employing diglycolamide (DGA) resins have shown the most promise~~proven effective~~ at separating Ba, Ra, and Ln~~lanthanide fission products~~ from ^{225}Ac [13-15]. A column of TEHDGA resin (branched DGA) removes ^{140}Ba and ^{223,224,225}Ra contamination with 6 M HNO_3, followed by elution of ^{225}Ac in 10 M HNO_3, but typically with breakthrough of 1% of ^{140}La with the ^{225}Ac fraction [11,15]. The remaining Ln are stripped as a group with 0.1 M HCl with no separation between the individual Ln elements. ~~However, a tunable resin that could provide an alternative to the DGA resin would be desirable, especially if that resin could deliver greater separation factors in less time than the generally slow DGA. Additionally,~~ Rrecovery and separation of adjacent Ln~~lanthanid~~ along with the separation of ^{225}Ac ~~es some of which are co-produced with 225Ac as fission products~~ would be beneficial, and alternatives to DGA resins are necessary to achieve this.~~; a prospect that current separation flow sheets that utilize DGA do not achieve.~~ The ~~lanthanide~~ Ln elements find a breadth of use in technology due to their electronic, optical, and magnetic properties [16,17]; a novel system that allows for a selective and efficient separation of adjacent ~~lanthanides~~ Ln would thus find utility for analytical purposes in science and technology. From an analytical perspective, the lighter Ln~~lanthanides~~ are key analytes in nuclear forensics [18]; a variety of radiolanthanides also have applications in nuclear medicine [19]. Medical applications of radiolanthanides necessitate the separation of the desired radiolanthanide from the irradiated target material that was used to produce it, and from additional parent/daughter radiolanthanides. The target materials and daughter products are typically adjacent Ln~~lanthanide~~ elements with similar chemistry, making these chemical separations particularly difficult. For example, ^{140}Nd ($t_{1/2}$ = 3.37 d) can be used for Auger therapy and decays to ^{140}Pr ($t_{1/2}$ = 3.39 min), followed by

Formatted: Font color: Red

Formatted: Not Superscript/ Subscript

Formatted: Highlight

decay to stable ^{140}Ce. Neodymium-140 is nominally produced via proton or deuteron irradiation of ^{141}Pr targets (the ^{141}Pr(p,2n)^{140}Nd and ^{141}Pr(d,3n)^{140}Nd reactions), or by the bombardment of ^{140}Ce with helium (the ^{140}Ce(^{3}He,3n)^{140}Nd and ^{140}Ce(^{4}He,4n)^{140}Nd reactions) [20]. Thus, the radiochemical separations required to produce a pure ^{140}Nd drug product entails its isolation from the adjacent Lnlanthanides ^{140}Ce and ^{140,141}Pr.

Ionic liquids (IL), more specifically Room Temperature Iionic Lliquids (RTIL), are promising alternatives for more traditional molecular solvents that are utilized in solvent extraction or chromatographic separation systems. Their low vapor pressure and flammability generally makes IL more environmentally friendly—"green"—solvents compared to harmful organic solvents and organophosphorus reagents which are ubiquitous in rare earth and nuclear fuel separations [21,22]. Ionic liquidsThey are capable of dissolving a variety of organic compounds and metal complexes, and it is straightforward to tune their chemistry for the desired separation application by modifying the cation/anion pair that makes up the IL, and/or using them as a diluent to incorporate extractant molecules with selectivity for the targeted metal(s). The IL/extractant solvent may be adsorbed on an inert stationary phase, such as a macro-porous polymeric resin, to produce a solvent impregnated resin (SIR) for use as a separations medium for extraction chromatography [23]. The IL solvent is physically adsorbed within porous polymer matrix, driven by favorable hydrophobic-hydrophobic interactions between the solvent and the resin [24]. This physical impregnation is straightforward, and can be accomplished by mixing a porous resin with the IL/extractant, followed by evaporation of excess solvent. TheseSuch IL based SIRs have been demonstrated in applications such as separation of Y(III) from other rare earth elements, and the separation of critical metals (Ln(III)lanthanides, In(III), Sn(IV)) from thin film leach solutions [254,265]. In particular, a SIR incorporating the IL,

1-butyl-3-methylimidazolium bis(trifluoromethylsulfonyl)imide ([Bmim][NTf_2]), and the diglycolamide extractant, *N*,*N*-dioctyldiglycolamic acid (DODGAA), has shown high efficiency for the separation of La(III) from other rare earth elements, Y(III), Eu(III), and Gd(III), by column elution with 2.5 M HNO_3 [265]. However, an exhaustive characterization of this SIR (furthermore notated as DODGAA/[Bmim][NTf_2]-SIR) for the adsorption of *f*-elements has not been undertaken. This would be of importance not only in the context of the development of efficient separations of accelerator produced ^{225}Ac from fission product Lnlanthanides, but also for the separation of adjacent Lnlanthanides for technological, analytical, and nuclear medicine applications.

In this work, the DODGAA/[Bmim][NTf_2]-SIR was prepared and investigated for the separation of ^{225}Ac from lanthanides (Ln), and the separation of adjacent Ln. Similar to a previous report [265], the resin was prepared with an Amberlite XAD7HP resin scaffold that was impregnated with [Bmim][NTf_2] and DODGAA to produce the DODGAA/[Bmim][NTf_2]-SIR (chemical structures of each component are displayed in Fig. 12). Batch extractions were performed to determine the equilibrium distribution coefficients of the rare earth elements (Sc(III), Y(III), Ln(III)), Th(IV), U(VI), and ^{225}Ac(III) in HCl and HNO_3 media to ascertain the adsorption affinity of these elements on the DODGAA/[Bmim][NTf_2]-SIR. Finally, dynamic column chromatography experiments were carried out to optimize the separations of ^{225}Ac from Ln and Ln from each other on the DODGAA/[Bmim][NTf_2]-SIR to provide a novel system for radiochemical, ^{225}Ac radionuclide production and broader analytical purposes.

2. Experimental

2.1. Materials

All chemicals were of reagent grade and aqueous solutions prepared with 18 $M\Omega \cdot cm^{-1}$ deionized water (Millipore). Nitric, hydrochloric, and hydrofluoric acids were purchased from Fisher Scientific (Pittsburgh, PA, USA) and were trace metal (Optima) grade. DODGAA (TCI America, Portland, OR, USA; >98%), [Bmim][NTf_2] (Sigma-Aldrich, St. Louis, MO, USA; ≥98%), AG1-X8 anion exchange resin (Bio-Rad, Hercules, CA, USA; 100-200 mesh, Cl^- form), branched DGA resin (Eichrom Technologies, Lisle, Il, USA; 50-100 µm), and pre-filter resin (Eichrom Technologies, Lisle, Il, USA; 100-150 µm) were used as received without further purification. Column experiments were performed using 0.8 × 4 cm Bio-Rad Poly-Prep chromatography columns which had stationary phase bed volume capacities of 2 mL, and 10 mL mobile phase reservoirs. Amberlite XAD7HP resin (Sigma-Aldrich, St. Louis, MO, USA) with a particle size of 560-710 µm (20-60 mesh), 0.5 $mL \cdot g^{-1}$ pore volume, a 0.03-0.04 µm pore size, and a surface area of 380 $m^2 \cdot g^{-1}$ was washed with 4 M HCl prior to preparing the SIR. Actinium-225 was separated from a ^{229}Th stock kept at Los Alamos that had earlier been obtained from the Oak Ridge National Laboratory (Oak Ridge, TN, USA). Multielement batch extractions and dynamic column experiments were carried out with BDH Aristar ICP rare earth metals group calibration standard which contained 100 $\mu g \cdot mL^{-1}$ of the following 18 elements in 7 wt% HNO_3: Sc, Y, La, Ce, Pr, Nd, Sm, Eu, Gd, Tb, Dy, Ho, Er, Tm, Yb, Lu, Th, and U (VWR, Radnor, PA, USA).

2.2. Instrumentation

High purity germanium (HPGe) gamma-ray spectrometry was used to quantify the radioactive components. An EG&G ORTEC Model GMX-35200-S HPGe combined with an ORTEC DSPEC 502 multichannel analyzer was used, and operated with GammaVision software (ORTEC, version 8.00.03). The detector diameter and length was 50.0 × 53.5 mm with a

0.5 mm beryllium detector window with an outer dead layer thickness of 0.3 μm. The system was initially calibrated against a standard radionuclide mixture of ^{57}Co, ^{60}Co, ^{88}Y, ^{109}Cd, ^{113}Sn, ^{137}Cs, ^{139}Ce, ^{203}Hg and ^{241}Am, traceable to the National Institute of Standards and Technology (NIST) and supplied by Eckert & Ziegler (Atlanta, GA, USA). Daily calibration checks were performed with a ^{152}Eu source (Eckert & Ziegler) which had the same counting geometry as the ^{225}Ac samples. Uncertainty in the total source activity ranged from 2.6 to 3.3% and counting dead times were kept below 10%.

The determination of Sc, Y, Ln (excluding Pm), Th, and U was accomplished by inductively coupled plasma atomic emission spectroscopy (ICP-AES) using a Shimadzu ICPE-9000. After a warmup time of a minimum of 30 min, the instrument was calibrated daily with calibration solutions prepared from BDH Aristar ICP rare earth metals group calibration standard in HCl or HNO_3 of the same acid concentration as the samples being analyzed. Triplicate readings with 30 s exposure times were collected for each sample. Atomic emission wavelengths were chosen to give the highest intensities while avoiding spectral interferences. Baseline corrections and data analysis were performed with ICPE Solutions software (Shimadzu Corp., version 1.01).

Attenuated total reflectance Fourier transform infrared (ATR-FTIR) spectra were collected for the unmodified Amberlite XAD7HP resin and the prepared DODGAA/[Bmim][NTf_2]-SIR. A Thermo Scientific Nicolet iS10 FTIR with a diamond crystal ATR-cell attachment was used to record the spectra of the dry resins, with data collection and analysis controlled with OMNIC FTIR software (Thermo Scientific, version 8.2.388). Spectra were collected at the range of 800-3200 cm^{-1}. Enough of the dry resin was added to cover the diamond crystal (~0.1 mg), lightly pressed down with the ATR-cell anvil, and 15 scans collected to record the ATR-FTIR spectrum. Background spectra were taken beforehand and subtracted from the sample spectra.

168 The diamond crystal was gently cleaned with ethanol and allowed to dry between samples. The
169 ATR-FTIR instrument was covered when not in use to prevent the accumulation of dust on the
170 crystal and optics.

171 *2.3. Isolation and preparation of ^{225}Ac*

172 Actinium-225 was isolated from a ^{229}Th stock by anion exchange and extraction
173 chromatography. A 1 mL column of AG1-X8 anion exchange resin was preconditioned three
174 times with 5 mL of water, and three times with 5 mL of 8 M HNO_3. A 5 mL solution of
175 ^{229}Th (5.8 MBq) in 8 M HNO_3 containing the daughter radionuclides ^{225}Ra and ^{225}Ac was loaded
176 onto the column and then washed with 5 mL of 8 M HNO_3, where ^{225}Ra and ^{225}Ac would pass
177 through the column while ^{229}Th was retained. The $^{225}Ra/^{225}Ac$ containing washes were diluted
178 with water to reach a HNO_3 concentration of 6 M, and loaded onto a 1 mL branched DGA resin
179 column that was preconditioned three times with 5 mL of water and three times with 5 mL of
180 6 M HNO_3. This column was washed twice with 5 mL of 6 M HNO_3 to remove ^{225}Ra while
181 retaining ^{225}Ac on the column. Actinium-225 was then eluted with eight, 5 mL portions of
182 0.05 M HNO_3, and the eluate was then passed through a 1 mL column of pre-filter resin to
183 remove trace organic compounds. The ^{225}Ac solution was finally evaporated to a residue under
184 gentle heating on a hot plate and dissolved in 6 mL of 0.01 M HNO_3.

185 *2.4. Preparation of DODGAA/[Bmim][NTf_2]-SIR*

186 DODGAA/[Bmim][NTf_2]-SIR was prepared following the methods reported in the
187 literature [265]. Approximately 60 mL of 4 M HCl was added to cover 30 g of Amberlite
188 XAD7HP and stirred for 2 hr. The HCl was decanted and the Amberlite washed with deionized
189 water until the pH of the rinsate was neutral to litmus. The washed Amberlite was then allowed
190 to dry overnight in a drying oven. Equal quantities of 1.500 g of DODGAA and [Bmim][NTf_2]

were combined and dissolved in 50 mL of acetone. The dry Amberlite (now a fine white powder) was allowed to cool to room temperature, after which 6 g was added to the DODGAA/[Bmim][NTf_2] solution and stirred for 24 hr. Finally, the acetone was removed by rotary evaporation at 40 °C.

2.5. Determination of the equilibrium distribution coefficients

The equilibrium distribution coefficients, K_d (mL·g^{-1}), of Sc(III), Y(III), Ln(III) (La-Lu exluding Pm), Th(IV), U(VI), and ^{225}Ac(III) on DODGAA/[Bmim][NTf_2]-SIR from 0.15 to 10 M solutions of HCl and HNO_3 were determined via batch extraction experiments. The K_d was calculated from:

$$K_d = \frac{C_{resin}}{C_{aq}} = \left(\frac{C_i - C_{eq}}{C_{eq}}\right) \cdot \left(\frac{V}{m}\right) \quad (1)$$

where C_{resin} and C_{aq} are the respective equilibrium concentrations of analyte in the resin phase and in the aqueous phase, C_i is the initial concentration (measured in a separate control experiment), C_{eq} is the concentration in the aqueous phase at equilibrium after contacting the resin, V is the volume of the aqueous phase (mL), and m is the mass of the resin (g). In the ^{225}Ac experiments, concentration was replaced by the measured count rate of the 218 keV and 440 keV gamma-ray emissions of its respective daughter radionuclides, ^{221}Fr and ^{213}Bi, after reaching radioactive equilibrium. Two mL centrifuge vials were loaded with 25 mg of DODGAA/[Bmim][NTf_2]-SIR and 1 mL of HCL or HNO_3 solution (varied acid concentration between 0.15 and 10 M) containing 10 mg·L^{-1} of the 18 element rare earth standard solution, or spiked with 10 kBq of ^{225}Ac. Five mL of the 18 element rare earth standard was first evaporated to dryness and redissolved in 5 mL of 0.1 M HCl for the experiments performed in HCl media. The two phases were mixed for 24 hr on a rocker (Thermo Scientific Labquake

212 Shaker/Rotisserie), after which the biphasic mixtures were passed through 0.45 μm PTFE
213 syringe filters to separate the resin from the aqueous phase. A 300 μL aliquot of the filtrate was
214 diluted to 10 mL to an acid concentration of 1 M HCl or HNO_3 for ICP-AES analysis to
215 determine the equilibrium concentration remaining in the aqueous phase. A 300 μL aliquot of
216 the filtrate was diluted to 5 mL and counted by HPGe for the ^{225}Ac experiments. These
217 experiments were repeated in triplicate.

218 *2.6. Column separations*

219 A series of dynamic column experiments were performed to develop two separation systems:
220 (1) the separation of adjacent Ln, and (2) the separation of ^{225}Ac from a mixture of Ln and ^{225}Ra.
221 In the first system, 0.6 g of DODGAA/[Bmim][NTf_2]-SIR was added to 10 M HNO_3 and slurry
222 packed to produce a column with a 2 mL wet resin bed with a gravity flow rate of
223 0.03 mL·min^{-1}. The column was washed three times with 5 mL of 10 M HNO_3 before loading
224 with a 2 mL solution of 5 mg·L^{-1} of the 18 element rare earth standard (containing Sc, Y, Ln, Th,
225 and U) in 10 M HNO_3. The column was then eluted in 2 mL fractions starting with 10 M HNO_3,
226 followed by gradient elution with decreasing concentrations of HNO_3 down to 3 M. The most
227 strongly retained elements on the DODGAA/[Bmim][NTf_2]-SIR column were eluted with 4 M
228 HCl/0.01 M HF. A 1 mL aliquot from each fraction was diluted to 5 mL to an acid concentration
229 of 1 M HCl or HNO_3 and analyzed by ICP-AES to determine the content of each metal in the
230 fraction.

231 For the second system, a 1 mL wet resin bed column of DODGAA/[Bmim][NTf_2]-SIR was
232 prepared in a similar manner by slurry packing 0.3 g of DODGAA/[Bmim][NTf_2]-SIR in 4 M
233 HCl, and then conditioning with three bed volumes of 4 M HCl. The gravity flow rate of this
234 column was 0.1 mL·min^{-1}. A 2 mL solution consisting of 5 mg·L^{-1} of the 18 element rare earth

standard, 5 kBq of ^{225}Ra, and 10 kBq of ^{225}Ac in 4 M HCl was loaded on the column and eluted with 4 M HCl in 2 mL fractions. Radium-225 was included to assess the Ra/Ac separation capability as well, because co-produced Ra isotopes are also contaminants in accelerator produced ^{225}Ac. Bismuth-213 (^{225}Ac decay product), ^{225}Ra, and La-Nd were eluted with 4 M HCl, after which ^{225}Ac was removed from the DODGAA/[Bmim][NTf_2]-SIR column and separated from the remaining Ln with 10 M HNO_3. Each fraction was analyzed for metal content by diluting 1 mL aliquots to 5 mL to an acid concentration of 1 M HCl or HNO_3, and then counted by HPGe to determine the radioactive components followed by ICP-AES for the stable elements. Degradation of the resin was not observed in either of the column separations. The DODGAA/[Bmim][NTf_2]-SIR columns were continually eluted over the course of a week while carrying out these experiments, without any change in column performance.

3. Results and discussion

3.1. ATR-FTIR spectra

The ATR-FTIR spectra of the Amberlite XAD7HP resin and the DODGAA/[Bmim][NTf_2]-SIR are shown in Fig. 2~~3~~. The primary features in the Amberlite XAD7HP spectrum include the carbonyl C=O stretch at 1724 cm^{-1} and the asymmetric C-O-C stretch at 1138 cm^{-1} from the ester groups in the resin polymer. New vibrational bands appear in the DODGAA/[Bmim][NTf_2]-SIR spectrum, after the Amberlite XAD7HP resin was impregnated with the DODGAA/[Bmim][NTf_2] solvent. The band~~s~~ at 2929 cm^{-1} and 1056 cm^{-1} represent~~s~~ the respective O-H and C-OH stretches in the carboxylic acid group of DODGAA, and match the values of 2925 and 1060 cm^{-1} that have been reported for the individual IR spectrum of DODGAA [27]. An aromatic C=C stretch from the cationic portion ($[Bmim]^+$) of the IL is visible at 1614 cm^{-1}. The bands from 1330 to 1350 cm^{-1} are attributed to the S=O

Formatted: Not Superscript/ Subscript

stretch, and the C-F stretch at 1182 cm^{-1} which are present in the anionic portion ($[NTf_2]^-$) of the IL; matching the designations listed in the Spectral Database for Organic Compounds, SDBS (https://sdbs.db.aist.go.jp/sdbs/cgi-bin/direct_frame_top.cgi) [28]. The band at 1056 cm^{-1} is assigned to the C-OH stretch from the carboxylic acid group in DODGAA. These spectra are an indication that the Amberlite XAD7HP starting material was modified and impregnated with DODGAA/[Bmim][NTf_2] by physisorption of the solvent in the pores of the resin; there is no evidence of chemisorption.

3.2. Equilibrium distribution coefficients

The determined equilibrium distribution coefficients for Sc(III), Y(III), Ln(III), ^{225}Ac(III), Th(IV), and U(VI) on DODGAA/[Bmim][NTf_2]-SIR from HCl and HNO_3 solutions are tabulated in Tables 1 and 2, and are displayed for select elements in Fig. 3 to maintain visual clarity while presenting the overall trends in these values.4, and the values are tabulated in Tables 1 and 2. Preliminary control experiments with unmodified Amberlite XAD7HP resin showed no measurable uptake of these elements; only on the DODGAA/[Bmim][NTf_2]-SIR did adsorption occur. In general, the maximum K_d values for Sc(III), Y(III), Ln(III), Th(IV), and U(VI) were observed at the lowest acid concentration studied (0.15 M) in both media. The K_d values were observed to decrease as the acid concentration was increased, reaching minimums at 4 M HCl and 3 M HNO_3, then followed by increasing adsorption up to 10 M acid. Measured K_d values for ^{225}Ac were generally an order of magnitude higher in HCl than in HNO_3 of the same concentration. The lowest affinity of ^{225}Ac(III) for the SIR was observed at 10 M HNO_3, in contrast with the other elements studied which tended to exhibit their near highest K_d values at this acid concentration—exceptions to this observation being La(III), Ce(III), Pr(III), and Nd(III).- Studies performed by Radchenko et al. have observed the preferential uptake of Ln(III)

over ^{225}Ac(III) by commercial DGA resins (same extractant class as the DODGAA extractant that was used to construct the SIR reported in this work) in the presence of nitrate ions [15]. The likely explanation is the formation of a ^{225}Ac(III) nitrate complex in the presence of high concentrations of nitrate ions that competes for the uptake by the DODGAA extractant in the SIR. Unfortunately, the nature of the coordination environment of the Ac^{3+} cation is minimally understood, with no data available in nitrate media to corroborate this observation [296,2,307].

The adsorption affinity of Ln(III) on DODGAA/[Bmim][NTf_2] can be correlated to the ionic radius, i.e. the charge density, of the Ln(III) cation. Shown in Fig. 45 are the K_d values for Ln(III) and Ac(III) on DODGAA/[Bmim][NTf_2]-SIR in HCl and HNO_3 as a function of the inverse ionic radius of the M^{3+} cation (ionic radii taken from Ref. [31~~28~~]). The K_d values increase following the lanthanide contraction showing a preference for the uptake of the heavier Ln(III) past Gd(III) after which the K_d values begin to plateau. This increase in the distribution coefficient with shrinking cation size (increasing charge density) along the lanthanide series is an indication of electrostatic interactions between the Ln^{3+} cation and the SIR, presumably with the oxygen-donor atoms on DODGAA. The implication of this observation is that DODGAA/[Bmim][NTf_2]-SIR exhibits selectivity for the uptake of the heavier Ln(III) while allowing for the separation of lighter Ln(III).

3.3. Separation of adjacent Ln by DODGAA/[Bmim][NTf_2]-SIR

The strategy for separating the Ln(III) elements was to load and elute with 10 M HNO_3 to remove the lightest Ln(III) elements, followed by gradient elution of decreasing HNO_3 concentration to sequentially elute heavier Ln(III) from the DODGAA/[Bmim][NTf_2]-SIR column. The elution profile for the Ln(III) elements on a 2 mL DODGAA/[Bmim][NTf_2]-SIR column is presented in Fig. 56. Lanthanum(III), Ce(III), and Pr(III) are eluted with 10 M HNO_3

with purities ($mg \cdot L^{-1}/mg \cdot L^{-1}$) of 94.2 ± 0.5%, 90.4 ± 0.5%, and 98.9 ± 0.1% respectively. Continued elution with 10 M HNO_3 would result in the elution of Nd(III), but in a broad band. Therefore, the elution matrix was changed to 6 M HNO_3 which removed pure Nd(III) in a fairly sharp band. Elution with 4 M HNO_3 removes Sm(III), Eu(III), and Gd(III). Highly pure 99.0 ± 0.2% Sm(III) is obtained, followed by Eu(III) at 93.8 ± 0.1% purity and Gd(III) at 82.6 ± 0.8% purity. Switching the elution matrix again to 3 M HNO_3 elutes Tb(III) with a fairly high purity of 95.2 ± 0.6%. Dysprosium(III) and Ho(III) are then removed, but the separation efficiencies of the heaviest Ln(III) begin to suffer due to continued band broadening and high distribution coefficients. The remaining Ln(III) on the column have reached their minimum K_d values at this acid concentration, but are still on the order of $K_d = 10^3$ $mL \cdot g^{-1}$. The heaviest Ln—Er(III), Tm(III), Yb(III), and Lu(III)—can be recovered from the column by eluting with 4 M HCl/0.01 M HF. This experiment was performed multiple times, and generally on a timeframe of a week (in practice these column separations can be completed in a day or two) with no changes in column performance when contacted with concentrated acids. Schaeffer et al. have described some losses of DODGAA and [Bmim][NTf_2] when regenerating and reusing a similar SIR over five cycles, but observed only a small decrease (<6%) in the absorption capacity for Y(III) [26]. While small losses of DODGAA/[Bmim][NTf_2] are likely occurring in our system, the time period and the reproducibility of these column experiments are not indicative of large leakages of DODGAA/[Bmim][NTf_2] from the resin that would have a dramatic effect on the separation.

The ability of DODGAA/[Bmim][NTf_2]-SIR to separate the light Ln(III) elements is useful in the context of separating Ce/Pr/Nd for production of ^{140}Nd for Auger therapy. The separation of ^{140}Nd from Ce and Pr targets has been demonstrated by cation exchange chromatography by

eluting with pH 4.7, 0.2-0.4 M α-hydroxyisobutyrate [32~~29~~,33~~0~~]. That procedure resulted in a small of amount of Ce or Pr overlap into the ^{140}Nd elution band, though typically >90% of pure ^{140}Nd was able to be recovered which is sufficient for continued radioisotope labeling studies. The procedure presented in this work on DODGAA/[Bmim][NTf_2]-SIR however, results in a completely clean Nd fraction. The primary advantage, however, is that the DODGAA/[Bmim][NTf_2]-SIR separation is free of additional complexing agents, such as α-hydroxyisobutyrate, that may interfere with radioisotope labeling for targeted therapy.

The elements Sc(III), Y(III), Th(IV), and U(VI) were also included in the loading mixture along with the Ln(III) elements, and their elution profile is shown in Fig. 6~~7~~. Surprisingly, U(VI) was eluted first from the column where it would have been expected to elute after Th(IV) based on the K_d values (Table 2). Uranium(VI) is present as the uranyl dioxocation $[O=U=O]^{2+}$ under these solution conditions, and the steric hindrance provided by the equatorial oxygen atoms might impede the chelation of UO_2^{2+} by the DODGAA/[Bmim][NTf_2] in the SIR. This could manifest itself by decreasing the complexation and extraction kinetics such that the equilibration of UO_2^{2+} on the DODGAA/[Bmim][NTf_2]-SIR is slower than the dynamic column flow, thus it is washed off the column in the first fractions. This is potentially advantageous, since it allows for rapid separation of U(VI) from Th(IV) with applications in geochemistry and nuclear forensics [34~~1~~-36~~3~~]. Yttrium(III) is separated from Sc(III) after elution with 3 M HNO_3.

3.4. Separation of ^{225}Ac from Ln by DODGAA/[Bmim][NTf_2]-SIR

The chromatographic separation of ^{225}Ac from Ln and ^{225}Ra is displayed in Fig. 7~~8~~. A 2 mL mixture of 5 mg·L^{-1} Ln(III) (La-Lu, excluding Pm), 5 kBq of ^{225}Ra(II), and 10 kBq of ^{225}Ac(III) was loaded onto a 1 mL DODGAA/[Bmim][NTf_2]-SIR column from 4 M HCl. The K_d values of Ln(III) are at their lowest values in 4 M HCl, while the value for ^{225}Ac(III) is relatively high at

$K_d = 10^{2.37\pm0.04}$ mL·g^{-1}. Elution with 20 mL of 4 M HCl removes La, Ce, Pr, and Nd, and also separates ^{213}Bi (^{225}Ac decay product) and ^{225}Ra. The elution matrix is then changed to 10 M HNO_3 to elute ^{225}Ac after these light Ln and radiochemical interferences are removed from the column. The first 2 mL fraction of 10 M HNO_3 elutes the remainder of Nd(III), followed by ^{225}Ac(III) which was collected in the next 8 mL of 10 M HNO_3 with a radiochemical yield of 101 ± 3%. The remainder of the Ln where retained on the column. Bismuth-213 and ^{223,224}Ra are alpha-emitters that also have application in TAT of cancer. Accelerator production of ^{225}Ac by proton irradiation of thorium targets results in the co-production of various Ra isotopes, namely ^{223,224,225}Ra, ^{213}Bi from the decay of ^{225}Ra/^{225}Ac, and lighterfission product Lnlanthanide fission productss such as ^{140}La, and ^{141,144}Ce, and ^{147}Nd [14,15]. In this context, ^{225}Ac needs to be isolated from Bi, Ra, and the lighter Ln elements, which can be accomplished with aA single column of DODGAA/[Bmim][NTf_2]-SIR. Additionally, this resin solves the challenge associated with breakthrough of ^{140}La with ^{225}Ac on branched DGA resin, because on the DODGAA/[Bmim][NTf_2]-SIR the light Ln are completely removed before ^{225}Ac. allows for the separation of Bi and Ra isotopes, as well as ^{225}Ac from Ln. After initial purification steps to remove bulk target material and other main group impurities, a DODGAA/[Bmim][NTf_2]-SIR column could be advantageous because it would also allow for the capture of these other valuable Bi and Ra isotopes during the radiochemical processing of accelerator produced ^{225}Ac.

3.5 Comparison with DGA Resins

Distribution coefficients for ^{225}Ac on TODGA (DGA) and TEHDGA (branched DGA) resins available from Eichrom Technologies have previously been determined by Radchenko et al., and values for 60 elements (including the rare earth elements, Th, and U) on TODGA resin have been determined by Pourmand and Dauphaus [15,374]. The former work measured a K_d value

for ^{225}Ac(III) on the order of 10^2 mL·g^{-1} in 6 M HNO_3 on TEHDGA resin, while the latter work indicated values generally >10^3 mL·g^{-1} for all the Ln (excluding Pr and Pm) throughout the acid range of 0.1 to 12 M HNO_3 on TODGA resin. As such, a facile separation of ^{225}Ac from Ln was possible using TEHDGA resin in 6 M HNO_3 with ^{225}Ac recovery yields of 98 ± 5% [15]. The DODGAA/[Bmim][NTf_2]-SIR reported here provides a comparable ^{225}Ac recovery yield as the TEHDGA resin. However, the K_d curves for Ln(III) in HNO_3 differ between the TODGA resin and the DODGAA/[Bmim][NTf_2]-SIR. All Ln(III) have K_d values >10^3 mL·g^{-1} across the acid range of 0.1 to 12 M HNO_3 on TODGA resin, while on the DODGAA/[Bmim][NTf_2]-SIR a 2-orders of magnitude difference in the K_d values between La(III) and Lu(III) is observed at a given concentration of HNO_3. This allows for the separation of Ln(III), the light Ln(III) in particular) in HNO_3 on DODGAA/[Bmim][NTf_2]-SIR with purities >90%. The case is similar between the two resins when comparing the data for HCl media where the Ln(III) display little variation in the K_d values across the series at a given HCl concentration on TODGA. The DODGAA/[Bmim][NTf_2]-SIR may serve as an alternative to the DGA resins in the separation of ^{225}Ac(III) from Ln(III), but has greater utility for the separation of adjacent Ln(III) elements compared to DGA. Studies in the future involving new combinations of ILs and extractants, including TODGA and TEHDGA, to produce new IL based SIRs will be explored in order to tune the extractability of *f*-elements, and to probe diluent effects that the IL itself may impart on the separation system.

4. Conclusion

The distribution and the column separations of Ln(III) and ^{225}Ac(III) ~~was~~ were investigated on a solvent impregnated resin incorporating the ionic liquid, [Bmim][NTf_2], and the extractant, DODGAA. The Ln(III) elements exhibited the highest uptake on the

DODGAA/[Bmim][NTf_2]-SIR from 0.15 M and 10 M solutions of HCl and HNO_3, and the lowest affinity for the SIR in 4 M HCl and 3 M HNO_3 respectively. The order of adsorption followed the lanthanide contraction independent of acid and concentration studied, with a selectivity of the heaviest Ln(III) over the lighter ones. Adsorption of ^{225}Ac (III) on DODGAA/[Bmim][NTf_2]-SIR differed from the Ln(III) in that the acid medium used notably changed the adsorption characteristics; K_d values in HCl were an order of magnitude larger than in HNO_3. These differences allowed for the development of column separations that separated Ln(III) from each other, and separated ^{225}Ac(III) from Ln(III). Purities generally >90% were obtained for the lighter Ln(III) without the addition of complexing agents in the elution medium, and may be suitable for the development of separations of ~~radiolanthanides~~ radioisotopes of lanthanides such as ^{140}Ce, ~~/~~ ^{140}Pr and ~~/~~ ^{140}Nd for nuclear medicine. Actinium-225 was separated from a mixture of Ln, ^{213}Bi, and ^{225}Ra quantitatively using only a single, 1 mL column of DODGAA/[Bmim][NTf_2]-SIR. This presents an alternative method of separating ^{225}Ac from Ra isotopes and fission product Ln~~lanthanides~~ that are produced from proton irradiation of thorium targets for making relevant quantities of ^{225}Ac for TAT. Further investigations of this SIR system with varied extractants and ILs are ongoing to tune the extraction characteristic to improve Ln(III) and ^{225}Ac(III) separations, and to better understand the role the IL diluent has on separations.

Declaration of competing interest

The authors declare that they have no known competing financial interests or personal relationships that could have appeared to influence the work reported in this paper.

Acknowledgments

This research was supported by the U.S. Department of Energy Isotope Program, managed by the Office of Science for Nuclear Physics.

References

[1] A. Morgenstern, C. Apostolidis, C. Kratochwil, M. Sathekge, L. Krolicki, F. Bruchertseifer, An Overview of Targeted Alpha Therapy with ^{225}Actinium and ^{213}Bismuth, Curr. Radiopharm. 11 (2018) 200-208.

[2] C. Apostolidis, R. Molinet, G. Rasmussen, A. Morgenstern, Production of Ac-225 from Th-229 for Targeted α Therapy, Anal. Chem. 77 (2005) 6288-6291.

[3] A.I. Kassis, Therapeutic Radionuclides: Biophysical and Radiobiologic Principles, Semin. Nucl. Med. 38 (2008) 358-366.

[4] M. Makvandi, E. Dupis, J.W. Engle, F.M. Nortier, M.E. Fassbender, S. Simon, E.R. Birnbaum, R.W. Atcher, K.D. John, O. Rixe, J.P. Norenberg, Alpha-Emitters and Targeted Alpha Therapy in Oncology: from Basic Science to Clinical Investigations, Target. Oncol. 13 (2018) 189-203.

[5] S. Kojima, J.M. Cuttler, N. Shimura, H. Koga, A. Murata, A. Kawashima, Present and Future Prospects of Radiation Therapy Using α-Emitting Nuclides, Dose Response 16 (2018) 1-8.

[6] C. Kratochwil, F. Bruchertseifer, F.L. Giesel, M. Weis, F.A. Verburg, F. Mottaghy, K. Kopka, C. Apostolidis, U. Haberkorn, A. Morgenstern, ^{225}Ac-PSMA-617 for PSMA-Targeted α-Radiation Therapy of Metastatic Castration-Resistant Prostate Cancer, J. Nucl. Med. 57 (2016) 1941-1944.

[7] R.A. Boll, D. Malkemus, S. Mirzadeh, Production of actinium-225 for alpha particle mediated radioimmunotherapy, Appl. Radiat. Isot. 62 (2005) 667-679.

[8] J.W. Engle, J.W. Weidner, B.D. Ballard, M.E. Fassbender, L.A. Hudston, K.R. Jackman, D.E. Dry, L.E. Wolfsberg, L.J. Bitteker, J.L. Ullmann, M.S. Gulley, C. Pillai, G. Goff, E.R. Birnbaum, K.D. John, S.G. Mashnik, F.M. Nortier, Ac, La, and Ce radioimpurities in ^{225}Ac produced in 40-200 MeV proton irradiations of thorium, Radiochim. Acta 102 (2014) 569-581.

[9] J.W. Weidner, S.G. Mashnik, K.D. John, F. Hemez, B. Ballard, H. Bach, E.R. Birnbaum, L.J. Bitteker, A. Couture, D. Dry, M.E. Fassbender, M.S. Gulley, K.R. Jackman, J.L. Ullmann, L.E. Wolfsberg, F.M. Nortier, Proton-induced cross sections relevant to production of ^{225}Ac and ^{223}Ra in natural thorium targets below 200 MeV, Appl. Radiat. Isot. 70 (2012) 2602-2607.

[10] J.R. Griswold, D.G. Medvedev, J.W. Engle, R. Copping, J.M. Fitzsimmons, V. Radchenko, J.C. Cooley, M.E. Fassbender, D.L. Denton, K.E. Murphy, A.C. Owens, E.R. Birnbaum, K.D. John, F.M. Nortier, D.W. Stracener, L.H. Heilbronn, L.F. Mausner, S. Mirzadeh, Large scale accelerator production of ^{225}Ac: Effective cross sections for 78-192 MeV protons incident on ^{232}Th targets, Appl. Radiat. Isot. 118 (2016) 366-374.

[11] V. Radchenko, J.W. Engle, J.J. Wilson, J.R. Maassen, F.M. Nortier, W.A. Taylor, E.R. Birnbaum, L.A. Hudston, K.D. John, M.E. Fassbender, Application of ion exchange and extraction chromatography to the separation of actinium from proton-irradiated thorium metal for analytical purposes, J. Chromatogr. A 1380 (2015) 55-63.

[12] D.R. McAlister, E.P. Horwitz, Selective separation or radium and actinium from bulk thorium target material on strong acid cation exchange resin from sulfate media, Appl. Radiat. Isot. 140 (2018) 18-23.

[13] B. Zielinska, C. Apostolidis, F. Bruchertseifer, A. Morgenstern, An Improved Method for the Production of Ac-225/Bi-213 from Th-229 for Targeted Alpha Therapy, Solv. Extr. Ion Exch. 25 (2007) 339-349.

[14] T. Mastren, V. Radchenko, A. Owens, R. Copping, R. Boll, J.R. Griswold, S. Mirzadeh, L.E. Wyant, M. Brugh, J.W. Engle, F.M. Nortier, E.R. Birnbaum, K.D. John, M.E. Fassbender, Simultaneous Separation of Actinium and Radium Isotopes from a Proton Irradiated Thorium Matrix, Scientific Reports 8216 (2017) 1-7.

[15] V. Radchenko, T. Mastren, C.A.L. Meyer, A.S. Ivanov, V.S. Bryantsev, R. Copping, D. Denton, J.W. Engle, J.R. Griswold, K. Murphy, J.J. Wilson, A. Owens, L. Wyant, E.R. Birnbaum, J. Fitzsimmons, D. Medvedev, C.S. Cutler, L.F. Mausner, M.F. Nortier, K.D. John, S. Mirzadeh, M.E. Fassbender, Radiometric evaluation of diglycolamide resins for the chromatographic separation of actinium from fission product lanthanides, Talanta 175 (2017) 318-324.

[16] J.-C.G. Bünzli, Benefiting from the Unique Properties of Lanthanide Ions, Acc. Chem. Res. 39 (2006) 53-61.

[17] K. Binnemans, Lanthanide-Based Luminescent Hybrid Materials, Chem. Rev. 109 (2009) 4283-4374.

[18] E. Keegan, M.J. Kristo, M. Colella, M. Robel, R. Williams, R. Lindvall, G. Eppich, S. Roberts, L. Borg, A. Gaffney, J. Plaue, H. Wong, J. Davis, E. Loi, M. Reinhard, I. Hutcheon, Nuclear forensic analysis of an

unknown uranium ore concentrate sample seized in a criminal investigation in Australia, Forensic Sci. Int. 240 (2014) 111-121.

[19] D. Nayak, S. Lahiri, Application of radioisotopes in the field of nuclear medicine I. Lanthanide series elements, J. Radioanal. Nucl. Chem. 242 (1999) 423-432.

[20] K. Hilgers, Y.N. Shubin, H.H. Coenen, S.M. Qaim, Experimental measurements and nuclear model calculations on the excitation functions of ^{nat}Ce(^{3}He,*xn*) and ^{141}Pr(*p*,*xn*) reactions with special reference to production of the therapeutic radionuclide ^{140}Nd, Radiochim. Acta 93 (2005) 553-560.

[21] J. Dehaudt, N.J. Williams, H. Luo, S. Dai, Extraction of Rare Earth in Ionic Liquids *Via* Competitive Ligand Complexation between TODGA and DTPA, Solvent Extr. Ion Exch. 36 (2018) 574-582.

[22] L. Qiu, Y. Pan, W. Zhang, A. Gong, Application of a functionalized ionic liquid extractant tributylmethylammonium dibutyldiglycolamate ([A336][BDGA]) in light rare earth extraction and separation, PLoS One 13 (2018) 1-13.

[23] C.A. Hawkins, Md.A. Momen, M.L. Dietz, Application of ionic liquids in the preparation of extraction chromatographic materials for metal ion separation: Progress and prospects, Sep. Sci. Technol. 53 (2018) 1820-1833.

~~[23]~~[24] N. Kabay, J.L. Cortina, A. Trochimczuk, M. Streat, Solvent-impregnated resins (SIRs) – Methods of preparation and their applications, React. Func. Polym. 70 (2010) 484-496.

~~[24]~~[25] X. Sun, B. Peng, Y. Ji, J. Chen, D. Li, The solid-liquid extraction of yttrium from rare earths by solvent (ionic liquid) impreganated resin coupled with complexing method, Sep. Purif. Techol. 63 (2008) 61-68.

[26] N. Schaeffer, S.M. Grimes, C.R. Cheeseman, Use of extraction chromatography in the recycling of critical metals from thin film leach solutions, Inorg. Chim. Acta 457 (2017) 53-58.

[27] R. Safarbali, M.R. Yaftian, A. Zamani, Solvent extraction-separation of La(III), Eu(III) and Er(III) ions from aqueous chloride medium using carbamoyl-carboxylic acid extractants, J. Rare Earths 34 (2016) 91-98.

~~[25]~~[28] Spectral Database for Organic Compounds, SDBS, https://sdbs.db.aist.go.jp/sdbs/cgi-bin/direct_frame_top.cgi (accessed 5 May 2020).

~~[26]~~[29] M.G. Ferrier, E.R. Batista, J.M. Berg, E.R. Birnbaum, J.N. Cross, J.W. Engle, H.S. La Pierre, S.A. Kozimor, J.S.L. Pacheco, B.W. Stein, C.E. Stieber, J.J. Wilson, Spectroscopic and computational investigation of actinium coordination chemistry, Nat. Commun. 12312 (2016) 1-8.

~~[27]~~[30] M.G. Ferrier, B.W. Stein, E.R. Batista, J.M. Berg, E.R. Birnbaum, J.W. Engle, K.D. John, S.A. Kozimer, J.S.L. Pacheco, L.N. Redman, Synthesis and Characterization of the Actinium Aquo Ion, ACS Cent. Sci. 3 (2017) 176-185.

~~[28]~~[31] R.D. Shannon, Revised Effective Ionic Radii and Systematic Studies of Interatomic Distances in Halides and Chalcogenides, Acta Cryst. A32 (1976) 751-767.

~~[29]~~[32] F. Rösch, J. Brockmann, N.A. Lebedev, S.M. Qaim, Production and Radiochemical Separation of the Auger Electron Emitter ^{140}Nd, Acta Oncologica 39 (2000) 727-730.

~~[30]~~[33] K.P. Zhernosekov, D.V. Filosofov, S.M. Qaim, F. Rösch, A ^{140}Nd/^{140}Pr radionuclide generator based on physico-chemical transitions in ^{140}Pr complexes after electron capture decay of ^{140}Nd-DOTA, Radiochim. Acta 95 (2007) 319-327.

~~[31]~~[34] J.-M. Gherardi, L. Labeyrie, S. Nave, R. Francois, J.F. McManus, E. Cortijo, Glacial-interglacial circulation changes inferred from ^{231}Pa/^{230}Th sedimentary record in the North Atlantic region, Paleoceanography, 24 (2009) 1-14.

~~[32]~~[35] M. Wallenius, A. Morgenstern, C. Apostolidis, K. Mayer, Determination of the age of highly enriched uranium, Anal. Bioanal. Chem. 374 (2002) 379-384.

~~[33]~~[36] F. Pointurier, A. Hubert, G. Roger, A method for dating small amounts of uranium, J. Radioanal. Nucl. Chem. 296 (2013) 593-598.

~~[34]~~[37] A. Pourmand, N. Dauphas, Distribution coefficients of 60 elements on TODGA resin: Application to Ca, Lu, Hf, U and Th isotope geochemistry, Talanta 81 (2010) 741-753.

List of Figures

~~**Fig. 1.** Decay scheme of ^{225}Ac.~~

Fig. 1~~2~~. Chemical structures of the components of the SIR.

Fig. 2~~3~~. ATR-FTIR spectra of Amberlite XAD7HP resin and the prepared DODGAA/[Bmim][NTf_2]-SIR. The * symbols indicate the appearance of new vibrational bands that arise after impregnation of the Amberlite XAD7HP with DODGAA/[Bmim][NTf_2].

Fig. 3~~4~~. K_d values (mL·g^{-1}) for select Ln(III) (other elements~~s~~ excluded for visual clarity), Y(III), ^{225}Ac(III), Th(IV), and U(VI) on DODGAA/[Bmim][NTf_2]-SIR in **a)** HCl and **b)** HNO_3. Error bars represent ±3σ from triplicates.

Fig. 4~~5~~. log K_d vs. the inverse ionic radius of Ln(III) (excluding Pm) and Ac(III) on DODGAA/[Bmim][NTf_2]-SIR in **a)** HCl and **b)** HNO_3 at acid concentrations of 2 M (■), 4 M (●), and 10 M (▲). Error bars represent ±3σ from triplicates. Ionic radii from Ref. [29~~8~~] (CN = 8 for Ln(III) and CN = 6 for Ac(III)).

Fig. 5~~6~~. Gradient elution profile for Ln(III) (excluding Pm) on a DODGAA/[Bmim][NTf_2]-SIR column. Column parameters: 0.8 × 4 cm column, 0.6 g resin, 2 mL resin bed volume, 0.03 mL·min^{-1} flow rate, 5 mg·L^{-1} each Ln(III).

Fig. 6~~7~~. Gradient elution profile for Sc(III), Y(III), Th(IV), and U(VI) on a DODGAA/[Bmim][NTf_2]-SIR column. Column parameters: 0.8 × 4 cm column, 0.6 g resin, 2 mL resin bed volume, 0.03 mL·min^{-1} flow rate, 5 mg·L^{-1} each of Sc(III), Y(III), Th(IV), and U(VI).

Fig. 7~~8~~. Chromatographic separation of ^{225}Ac(III) from Ln(III) on a DODGAA/[Bmim][NTf_2]-SIR column. Column parameters: 0.8 × 4 cm column, 0.3 g resin, 1 mL resin bed volume, 0.1 mL·min^{-1} flow rate, 5 mg·L^{-1} La-Lu (excluding Pm) each and spiked with 5 kBq of ^{225}Ra(II) and 10 kBq of ^{225}Ac(III).

List of Tables

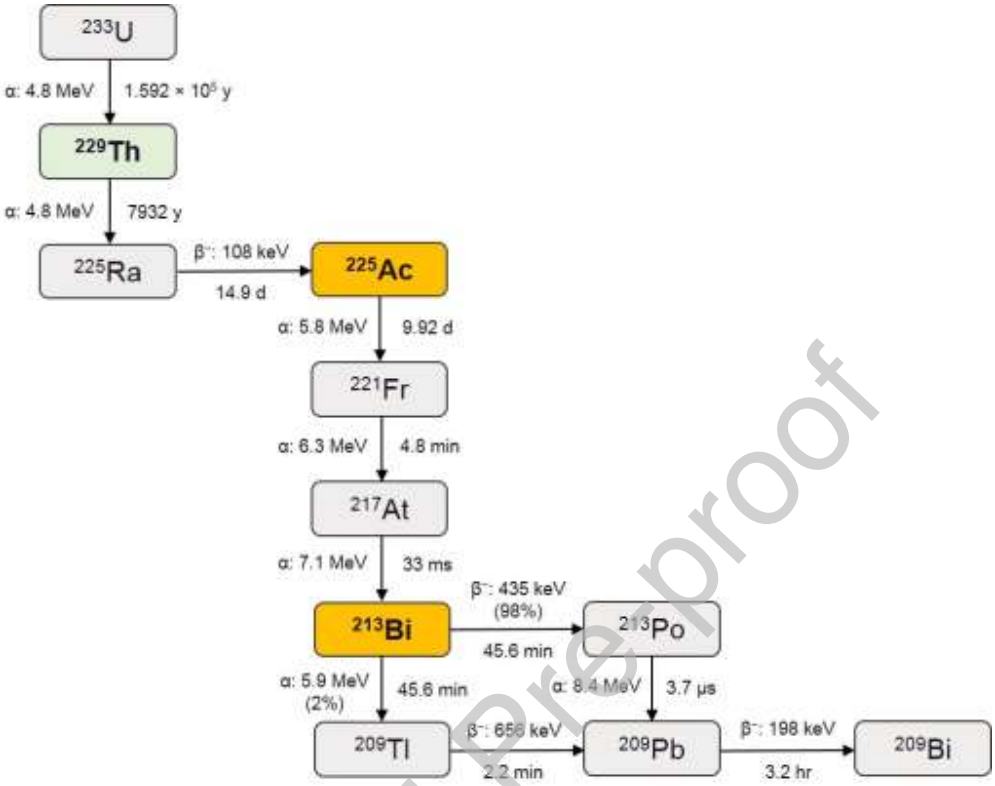

Fig. 1. Decay scheme of ^{225}Ac.

Formatted: Font: (Default) Times New Roman, 12 pt

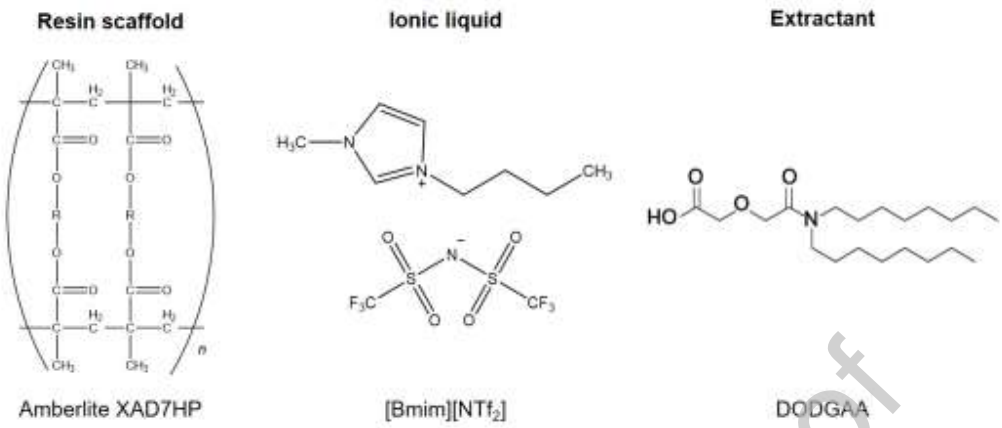

Fig. 12. Chemical structures of the components of the solvent impregnated resin.

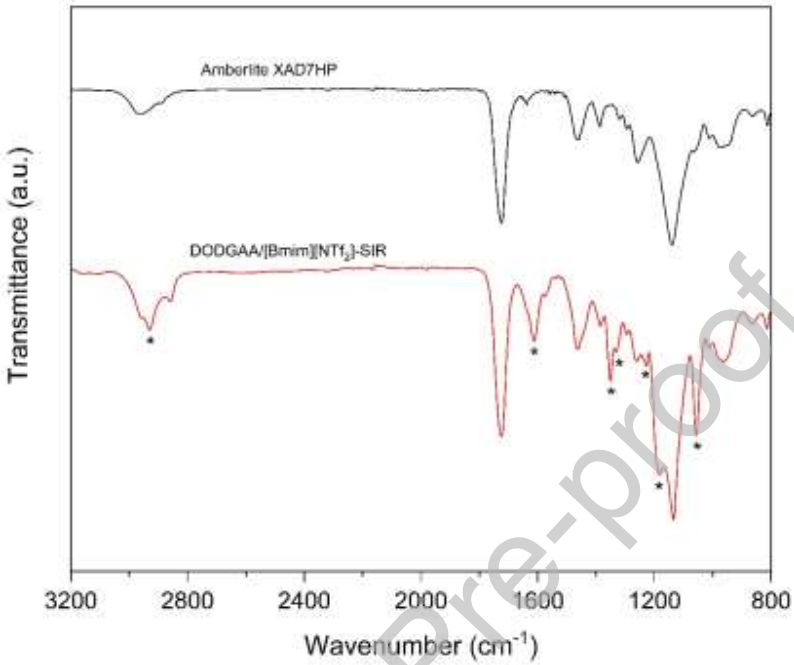

Fig. 23. ATR-FTIR spectra of Amberlite XAD7HP resin and the prepared DODGAA/[Bmim][NTf_2]-SIR. The * symbols indicate the appearance of new vibrational bands that arise after impregnation of the Amberlite XAD7HP with DODGAA/[Bmim][NTf_2].

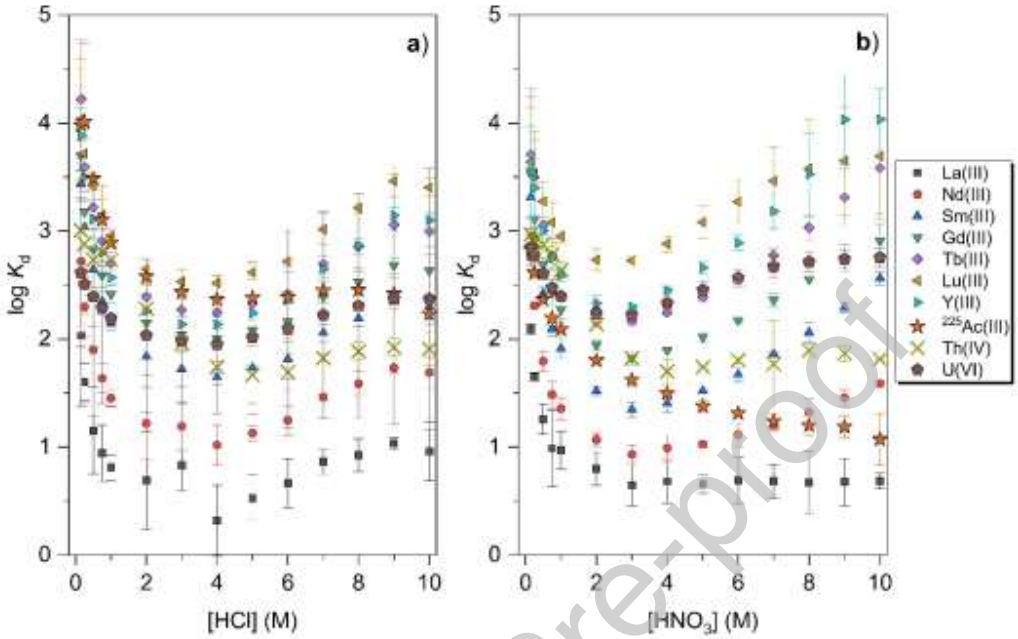

Fig. 34. K_d values (mL·g^{-1}) for select Ln(III) (other elements excluded for visual clarity), Y(III), ^{225}Ac(III), Th(IV), and U(VI) on DODGAA/[Bmim][NTf_2]-SIR in **a)** HCl and **b)** HNO_3. Error bars represent ±3σ from triplicates.

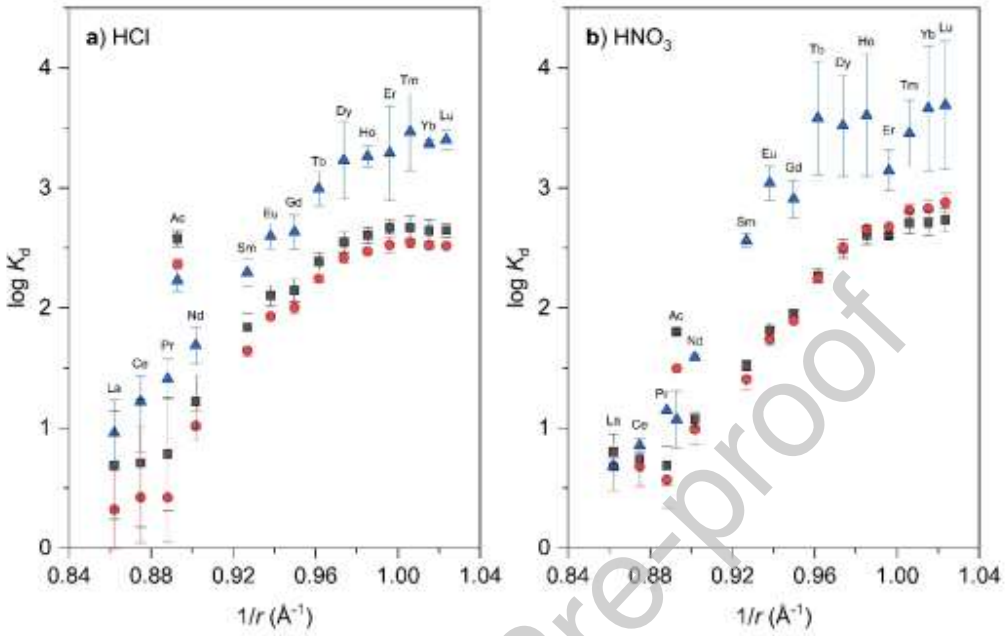

Fig. 45. log K_d vs. the inverse ionic radius of Ln(III) (excluding Pm) and Ac(III) on DODGAA/[Bmim][NTf_2]-SIR in **a)** HCl and b**)** HNO_3 at acid concentrations of 2 M (■), 4 M (●), and 10 M (▲). Error bars represent ±3σ from triplicates. Ionic radii from Ref. [298] (CN = 8 for Ln(III) and CN = 6 for Ac(III)).

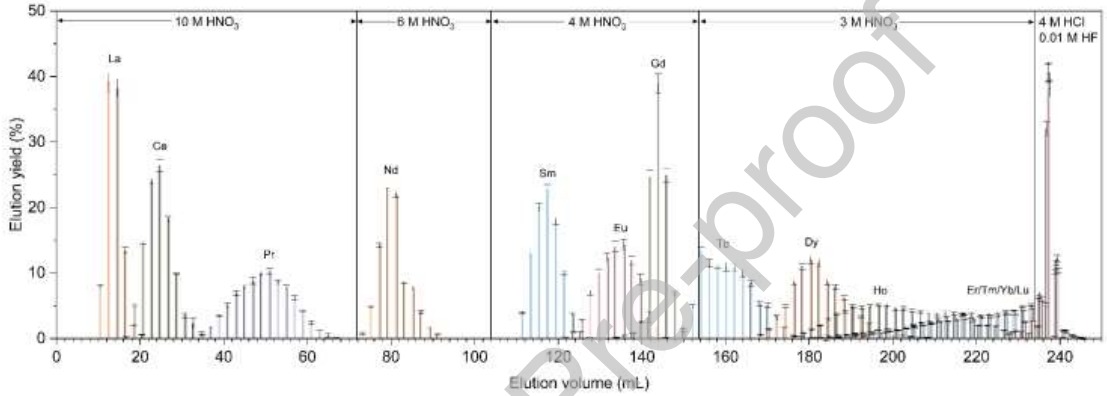

Fig. 56. Gradient elution profile for Ln(III) (excluding Pm) on a DODGAA/[Bmim][NTf_2]-SIR column. Column parameters: 0.8 × 4 cm column, 0.6 g resin, 2 mL resin bed volume, 0.03 mL·min^{-1} flow rate, 5 mg·L^{-1} each Ln(III).

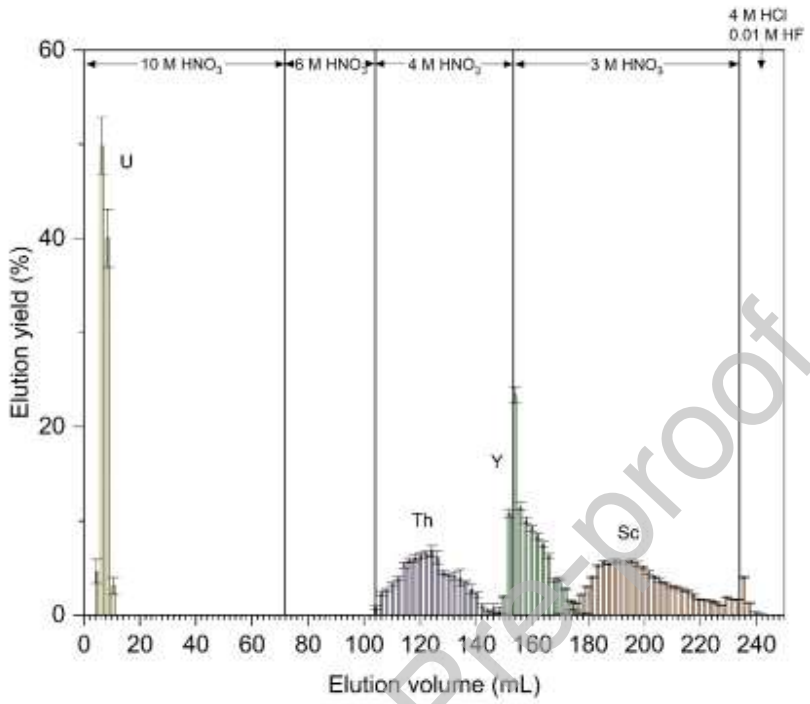

Fig. 67. Gradient elution profile for Sc(III), Y(III), Th(IV), and U(VI) on a DODGAA/[Bmim][NTf_2]-SIR column. Column parameters: 0.8 × 4 cm column, 0.6 g resin, 2 mL resin bed volume, 0.03 mL·min^{-1} flow rate, 5 mg·L^{-1} each of Sc(III), Y(III), Th(IV), and U(VI).

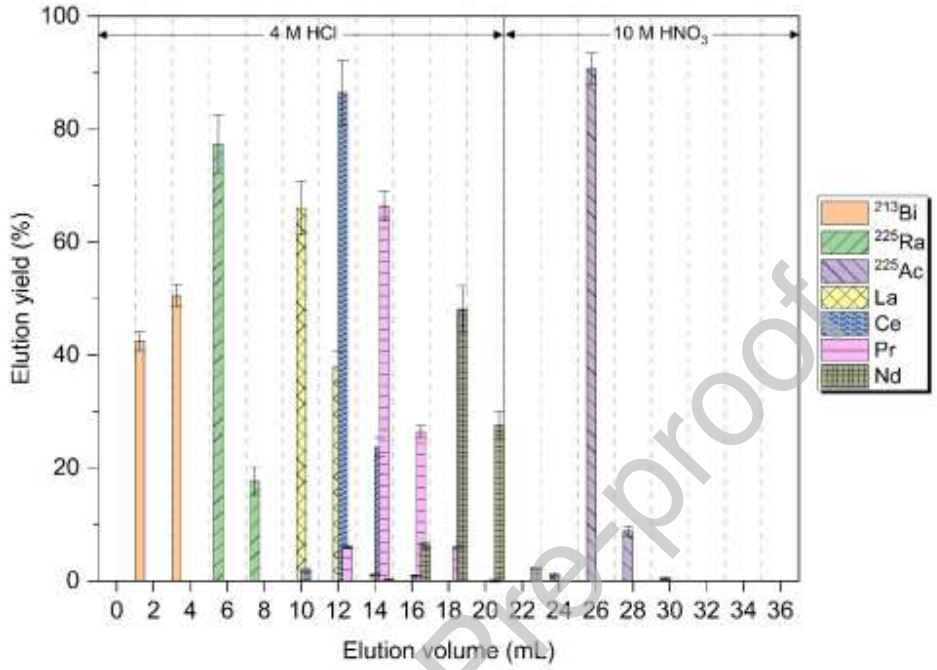

Fig. 78. Chromatographic separation of ^{225}Ac(III) from Ln(III) on a DODGAA/[Bmim][NTf_2]-SIR column. Column parameters: 0.8 × 4 cm column, 0.3 g resin, 1 mL resin bed volume, 0.1 mL·min^{-1} flow rate, 5 mg·L^{-1} La-Lu (excluding Pm) each and spiked with 5 kBq of ^{225}Ra(II) and 10 kBq of ^{225}Ac(III).

583 **Table 1**

584 Equilibrium distribution coefficients for Sc(III), Y(III), Ln(III), ^{225}Ac(III), Th(IV), and U(VI) on DODGAA/[Bmim][NTf_2]-SIR in HCl.

[HCl] (M)	K_d /mL·g^{-1} (values and uncertainties reported in $\log_{10}$ unit)[a]									
	La^{3+}	Ce^{3+}	Pr^{3+}	Nd^{3+}	Sm^{3+}	Eu^{3+}	Gd^{3+}	Tb^{3+}	Dy^{3+}	Ho^{3+}
0.15	2.0 ± 0.1	2.3 ± 0.1	2.63 ± 0.06	2.7 ± 0.1	3.4 ± 0.1	3.8 ± 0.2	3.7 ± 0.1	4.2 ± 0.5	4.4 ± 0.3	3.9 ± 0.3
0.25	1.6 ± 0.2	1.8 ± 0.3	2.1 ± 0.3	2.3 ± 0.3	3.0 ± 0.3	3.3 ± 0.3	3.2 ± 0.3	3.6 ± 0.4	3.7 ± 0.3	3.6 ± 0.2
0.50	1.2 ± 0.4	1.3 ± 0.4	1.6 ± 0.3	1.9 ± 0.2	2.6 ± 0.2	2.9 ± 0.2	2.8 ± 0.2	3.2 ± 0.2	3.4 ± 0.4	3.33 ± 0.08
0.75	0.9 ± 0.3	1.0 ± 0.2	1.3 ± 0.3	1.6 ± 0.1	2.3 ± 0.1	2.6 ± 0.1	2.6 ± 0.1	2.9 ± 0.1	3.06 ± 0.07	3.1 ± 0.1
1	0.8 ± 0.1	0.9 ± 0.2	1.1 ± 0.1	1.45 ± 0.07	2.15 ± 0.06	2.41 ± 0.06	2.41 ± 0.08	2.70 ± 0.07	2.9 ± 0.1	2.891 ± 0.005
2	0.7 ± 0.5	0.7 ± 0.3	0.8 ± 0.7	1.2 ± 0.3	1.8 ± 0.2	2.1 ± 0.1	2.1 ± 0.1	2.4 ± 0.1	2.5 ± 0.1	2.6 ± 0.1
3	0.8 ± 0.2	0.9 ± 0.3	0.8 ± 0.3	1.2 ± 0.2	1.7 ± 0.2	2.0 ± 0.1	2.0 ± 0.2	2.3 ± 0.1	2.4 ± 0.2	2.5 ± 0.1
4	0.2 ± 0.3	0.4 ± 0.2	0.4 ± 0.4	1.0 ± 0.2	1.64 ± 0.07	1.93 ± 0.04	2.00 ± 0.08	2.24 ± 0.04	2.42 ± 0.06	2.47 ± 0.02
5	0.5 ± 0.2	0.7 ± 0.2	0.7 ± 0.1	1.13 ± 0.07	1.73 ± 0.02	2.01 ± 0.04	2.08 ± 0.01	2.33 ± 0.05	2.51 ± 0.03	2.56 ± 0.06
6	0.7 ± 0.2	0.8 ± 0.3	0.9 ± 0.1	1.2 ± 0.1	1.8 ± 0.2	2.1 ± 0.2	2.2 ± 0.2	2.4 ± 0.3	2.6 ± 0.3	2.7 ± 0.3
7	0.9 ± 0.1	1.05 ± 0.03	1.16 ± 0.06	1.46 ± 0.03	2.06 ± 0.08	2.34 ± 0.09	2.39 ± 0.06	2.69 ± 0.08	2.89 ± 0.03	2.9 ± 0.1
8	0.9 ± 0.2	1.1 ± 0.2	1.30 ± 0.09	1.6 ± 0.1	2.19 ± 0.07	2.48 ± 0.05	2.5 ± 0.1	2.85 ± 0.07	3.1 ± 0.1	3.10 ± 0.04
9	1.03 ± 0.06	1.28 ± 0.07	1.47 ± 0.03	1.73 ± 0.05	2.35 ± 0.04	2.65 ± 0.03	2.68 ± 0.07	3.06 ± 0.05	3.3 ± 0.1	3.3 ± 0.1
10	1.0 ± 0.3	1.2 ± 0.2	1.4 ± 0.2	1.7 ± 0.1	2.3 ± 0.1	2.6 ± 0.1	2.6 ± 0.1	3.0 ± 0.1	3.2 ± 0.3	3.26 ± 0.09

[HCl] (M)	Er^{3+}	Tm^{3+}	Yb^{3+}	Lu^{3+}	Sc^{3+}	Y^{3+}	$^{225}Ac^{3+}$	Th^{4+}	UO_2^{2+}	
0.15	4.2 ± 0.6	4.0 ± 0.6	4.0 ± 0.4	4.0 ± 0.6	3.9 ± 0.2	3.9 ± 0.3	4.0 ± 0.5	3.0 ± 0.3	3 ± 1	
0.25	3.7 ± 0.4	3.7 ± 0.1	3.7 ± 0.3	3.7 ± 0.2	3.7 ± 0.3	3.5 ± 0.4	4.0 ± 0.7	2.9 ± 0.6	3 ± 1	
0.50	3.4 ± 0.3	3.5 ± 0.5	3.40 ± 0.04	3.42 ± 0.04	3.50 ± 0.05	3.1 ± 0.2	3.48 ± 0.05	2.7 ± 0.8	2 ± 1	
0.75	3.1 ± 0.3	3.18 ± 0.08	3.1 ± 0.2	3.2 ± 0.1	3.3 ± 0.1	2.8 ± 0.1	3.1 ± 0.3	2.8 ± 0.1	2.3 ± 0.9	
1	2.9 ± 0.1	3.0 ± 0.1	2.94 ± 0.02	2.95 ± 0.02	3.07 ± 0.03	2.57 ± 0.06	2.89 ± 0.09	2.7 ± 0.1	2.2 ± 0.8	
2	2.67 ± 0.09	2.7 ± 0.1	2.6 ± 0.1	2.65 ± 0.08	2.8 ± 0.1	2.3 ± 0.2	2.58 ± 0.07	2.3 ± 0.1	2.0 ± 0.7	
3	2.6 ± 0.1	2.6 ± 0.2	2.52 ± 0.09	2.5 ± 0.1	2.7 ± 0.1	2.1 ± 0.1	2.43 ± 0.06	1.96 ± 0.07	2.0 ± 0.6	
4	2.5 ± 0.1	2.54 ± 0.07	2.52 ± 0.03	2.52 ± 0.02	2.64 ± 0.07	2.13 ± 0.03	2.37 ± 0.04	1.74 ± 0.05	1.9 ± 0.6	
5	2.6 ± 0.1	2.64 ± 0.04	2.62 ± 0.03	2.62 ± 0.07	2.76 ± 0.01	2.24 ± 0.02	2.4 ± 0.2	1.7 ± 0.3	2.0 ± 0.7	
6	2.7 ± 0.2	2.8 ± 0.3	2.7 ± 0.2	2.7 ± 0.3	2.9 ± 0.2	2.4 ± 0.3	2.4 ± 0.3	1.7 ± 0.2	2.1 ± 0.9	
7	3.0 ± 0.4	3.04 ± 0.07	3.0 ± 0.1	3.0 ± 0.1	3.12 ± 0.07	2.65 ± 0.07	2.45 ± 0.08	1.82 ± 0.03	2 ± 1	
8	3.2 ± 0.4	3.2 ± 0.1	3.18 ± 0.06	3.21 ± 0.05	3.2 ± 0.1	2.86 ± 0.02	2.5 ± 0.2	1.88 ± 0.09	2 ± 1	
9	3.4 ± 0.5	3.5 ± 0.2	3.4 ± 0.1	3.5 ± 0.1	3.33 ± 0.05	3.15 ± 0.07	2.4 ± 0.1	1.92 ± 0.08	2 ± 1	
10	3.3 ± 0.4	3.5 ± 0.3	3.37 ± 0.03	3.40 ± 0.08	3.27 ± 0.06	3.10 ± 0.07	2.2 ± 0.1	1.9 ± 0.2	2 ± 1	

585 [a]Uncertainties reported as ±3σ from triplicates

586 **Table 2**
587 Equilibrium distribution coefficients for Sc(III), Y(III), Ln(III), ^{225}Ac(III), Th(IV), and U(VI) on DODGAA/[Bmim][NTf_2]-SIR in HNO_3.

$[HNO_3]$ (M)	K_d /mL·g^{-1} (values and uncertainties reported in $\log_{10}$ unit)[a]									
	La^{3+}	Ce^{3+}	Pr^{3+}	Nd^{3+}	Sm^{3+}	Eu^{3+}	Gd^{3+}	Tb^{3+}	Dy^{3+}	Ho^{3+}
0.15	2.09 ± 0.05	2.33 ± 0.05	2.64 ± 0.04	2.76 ± 0.04	3.3 ± 0.3	3.5 ± 0.3	3.5 ± 0.7	3.7 ± 0.6	3.6 ± 0.5	3.6 ± 0.4
0.25	1.65 ± 0.04	1.83 ± 0.04	2.10 ± 0.04	2.31 ± 0.04	2.95 ± 0.09	3.2 ± 0.2	3.1 ± 0.3	3.5 ± 0.3	3.5 ± 0.4	3.5 ± 0.4
0.50	1.3 ± 0.1	1.3 ± 0.1	1.5 ± 0.1	1.79 ± 0.09	2.42 ± 0.07	2.69 ± 0.04	2.69 ± 0.06	3.05 ± 0.08	3.1 ± 0.1	3.2 ± 0.1
0.75	1.0 ± 0.4	1.0 ± 0.3	1.2 ± 0.2	1.5 ± 0.1	2.09 ± 0.08	2.38 ± 0.08	2.4 ± 0.1	2.8 ± 0.1	2.9 ± 0.1	3.0 ± 0.2
1	1.0 ± 0.2	0.9 ± 0.2	1.0 ± 0.2	1.4 ± 0.1	1.91 ± 0.09	2.19 ± 0.08	2.27 ± 0.09	2.60 ± 0.07	2.78 ± 0.06	2.86 ± 0.05
2	0.8 ± 0.2	0.7 ± 0.1	0.7 ± 0.2	1.07 ± 0.06	1.52 ± 0.04	1.82 ± 0.05	1.94 ± 0.04	2.27 ± 0.06	2.49 ± 0.07	2.61 ± 0.08
3	0.6 ± 0.2	0.6 ± 0.1	0.5 ± 0.2	0.93 ± 0.09	1.35 ± 0.07	1.68 ± 0.04	1.83 ± 0.07	2.16 ± 0.04	2.41 ± 0.03	2.55 ± 0.03
4	0.7 ± 0.2	0.7 ± 0.2	0.6 ± 0.2	1.0 ± 0.1	1.41 ± 0.09	1.74 ± 0.05	1.89 ± 0.01	2.25 ± 0.03	2.51 ± 0.03	2.66 ± 0.04
5	0.66 ± 0.08	0.66 ± 0.07	0.62 ± 0.09	1.03 ± 0.03	1.52 ± 0.01	1.858 ± 0.009	2.02 ± 0.05	2.39 ± 0.03	2.65 ± 0.06	2.81 ± 0.08
6	0.7 ± 0.2	0.7 ± 0.2	0.7 ± 0.2	1.1 ± 0.1	1.67 ± 0.07	2.02 ± 0.04	2.17 ± 0.03	2.56 ± 0.03	2.82 ± 0.05	2.98 ± 0.09
7	0.7 ± 0.2	0.7 ± 0.1	0.8 ± 0.1	1.21 ± 0.06	1.86 ± 0.02	2.219 ± 0.003	2.36 ± 0.06	2.78 ± 0.06	3.0 ± 0.1	3.2 ± 0.2
8	0.7 ± 0.3	0.7 ± 0.2	0.9 ± 0.3	1.3 ± 0.1	2.06 ± 0.09	2.44 ± 0.08	2.55 ± 0.03	3.0 ± 0.1	3.2 ± 0.2	3.4 ± 0.2
9	0.7 ± 0.2	0.8 ± 0.2	1.0 ± 0.1	1.45 ± 0.07	2.29 ± 0.05	2.71 ± 0.08	2.7 ± 0.1	3.3 ± 0.3	3.4 ± 0.3	3.5 ± 0.4
10	0.68 ± 0.07	0.85 ± 0.06	1.15 ± 0.02	1.59 ± 0.03	2.56 ± 0.06	3.0 ± 0.1	2.9 ± 0.2	3.6 ± 0.5	3.5 ± 0.4	3.6 ± 0.5

$[HNO_3]$ (M)	Er^{3+}	Tm^{3+}	Yb^{3+}	Lu^{3+}	Sc^{3+}	Y^{3+}	$^{225}Ac^{3+}$	Th^{4+}	UO_2^{2+}
0.15	3.1 ± 0.2	3.5 ± 0.3	3.6 ± 0.5	3.6 ± 0.5	3.5 ± 0.4	3.6 ± 0.4	2.8 ± 0.1	2.97 ± 0.02	2.9 ± 0.2
0.25	3.1 ± 0.2	3.4 ± 0.3	3.5 ± 0.4	3.5 ± 0.4	3.5 ± 0.3	3.4 ± 0.3	2.61 ± 0.06	2.90 ± 0.09	2.8 ± 0.1
0.50	2.9 ± 0.1	3.2 ± 0.1	3.3 ± 0.2	3.3 ± 0.2	3.3 ± 0.2	3.00 ± 0.04	2.37 ± 0.07	2.87 ± 0.07	2.60 ± 0.04
0.75	2.9 ± 0.1	3.0 ± 0.1	3.1 ± 0.2	3.1 ± 0.2	3.1 ± 0.2	2.7 ± 0.1	2.19 ± 0.03	2.8 ± 0.1	2.47 ± 0.08
1	2.8 ± 0.1	2.92 ± 0.05	2.93 ± 0.05	2.95 ± 0.07	2.91 ± 0.05	2.59 ± 0.06	2.09 ± 0.07	2.64 ± 0.07	2.40 ± 0.03
2	2.60 ± 0.01	2.71 ± 0.09	2.7 ± 0.1	2.7 ± 0.1	2.53 ± 0.06	2.33 ± 0.07	1.80 ± 0.02	2.14 ± 0.02	2.2 ± 0.1
3	2.58 ± 0.01	2.69 ± 0.03	2.69 ± 0.03	2.73 ± 0.04	2.32 ± 0.02	2.30 ± 0.03	1.62 ± 0.06	1.82 ± 0.03	2.22 ± 0.04
4	2.68 ± 0.05	2.82 ± 0.04	2.83 ± 0.08	2.88 ± 0.07	2.27 ± 0.04	2.45 ± 0.04	1.50 ± 0.01	1.7 ± 0.1	2.33 ± 0.08
5	2.81 ± 0.08	2.98 ± 0.08	3.0 ± 0.1	3.1 ± 0.1	2.27 ± 0.03	2.66 ± 0.06	1.38 ± 0.06	1.74 ± 0.01	2.45 ± 0.08
6	2.90 ± 0.09	3.12 ± 0.07	3.2 ± 0.2	3.3 ± 0.2	2.30 ± 0.03	2.89 ± 0.07	1.31 ± 0.02	1.80 ± 0.03	2.56 ± 0.08
7	3.0 ± 0.2	3.3 ± 0.1	3.2 ± 0.2	3.5 ± 0.3	2.391 ± 0.009	3.2 ± 0.2	1.24 ± 0.07	1.8 ± 0.4	2.7 ± 0.1
8	3.1 ± 0.2	3.4 ± 0.2	3.5 ± 0.4	3.6 ± 0.4	2.51 ± 0.07	3.5 ± 0.4	1.20 ± 0.09	1.89 ± 0.06	2.71 ± 0.09
9	3.1 ± 0.1	3.4 ± 0.2	3.6 ± 0.4	3.7 ± 0.5	2.67 ± 0.07	4.0 ± 0.4	1.2 ± 0.1	1.87 ± 0.07	2.74 ± 0.09
10	3.1 ± 0.2	3.5 ± 0.3	3.7 ± 0.5	3.7 ± 0.5	2.85 ± 0.09	4.0 ± 0.3	1.1 ± 0.2	1.81 ± 0.01	2.75 ± 0.09

588 [a]Uncertainties reported as ±3σ from triplicates